Gb/s Underwater Wireless Optical Communications Using Series-Connected GaN Micro-LED Arrays

Gb/s Underwater Wireless Optical Communications Using Series-Connected GaN Micro-LED Arrays

Georgios N. Arvanitakis
Rui Bian
Jonathan J. D. McKendry
Chen Cheng
Enyuan Xie
Xiangyu He
Gang Yang
Mohamed S. Islim
Ardimas A. Purwita
Erdan Gu, *Member, IEEE*
Harald Haas, *Fellow, IEEE*
Martin D. Dawson, *Fellow, IEEE*
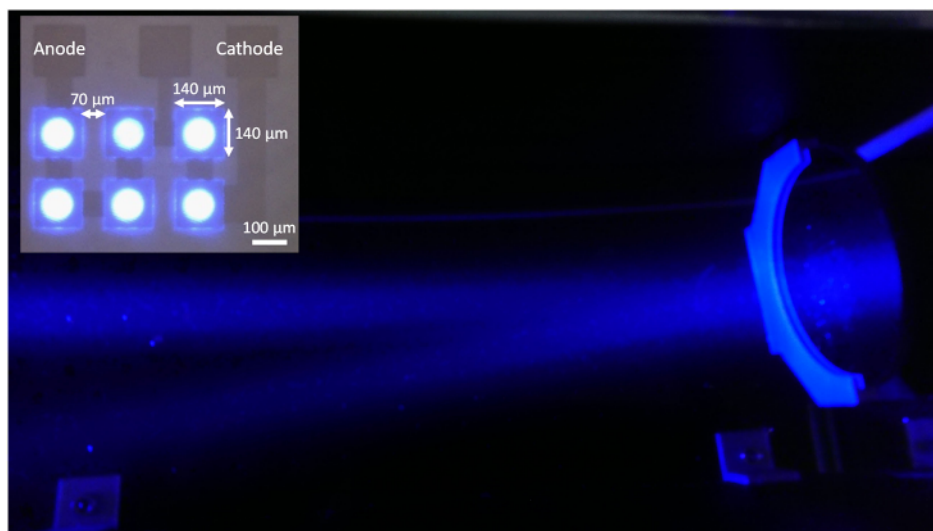
Gb/s Underwater Wireless Optical Communications Using Series-Connected GaN Micro-LED Arrays

Georgios N. Arvanitakis [iD],[1] **Rui Bian** [iD],[2]
Jonathan J. D. McKendry [iD],[1] **Chen Cheng** [iD],[2] **Enyuan Xie** [iD],[1]
Xiangyu He [iD],[1] **Gang Yang**,[3] **Mohamed S. Islim** [iD],[2]
Ardimas A. Purwita [iD],[2] **Erdan Gu**,[1] *Member, IEEE*,
Harald Haas [iD],[2] *Fellow, IEEE*,
and **Martin D. Dawson** [iD],[1] *Fellow, IEEE*

[1]Institute of Photonics, Department of Physics, SUPA, University of Strathclyde, Glasgow
G1 1RD, U.K.
[2]Li-Fi R&D Centre, Institute for Digital Communications, University of Edinburgh, Edinburgh
EH9 3JL, U.K.
[3]Institute of Marine Optoelectronic Equipment, Harbin Institute of Technology, WeiHai
264209, China

Abstract: High speed wireless communications are highly desirable for many industrial and scientific underwater applications. Acoustic communications suffer from high latency and limited data rates, while Radio Frequency communications are severely limited by attenuation in seawater. Optical communications are a promising alternative, offering high transmission rates (up to Gb/s), while water has relatively low attenuation at visible wavelengths. Here we demonstrate the use of series-connected micro-light-emitting-diode (μLED) arrays consisting of 6 μLED pixels either 60 μm or 80 μm in diameter and operating at 450 nm. These devices increase the output power whilst maintaining relatively high modulation bandwidth. Using orthogonal frequency division multiplexing (OFDM) we demonstrate underwater wireless data transmission at rates of up to 4.92 Gb/s, 3.22 Gb/s and 3.4 Gb/s over 1.5 m, 3 m and 4.5 m, respectively, with corresponding bit error ratios (BERs) of 1.5×10^{-3}, 1.1×10^{-3} and 3.1×10^{-3}, through clear tap water, and Mb/s rates through >5 attenuation lengths (ALs) in turbid waters.

Index Terms: GaN, micro-light-emitting-diode arrays, turbid waters, underwater wireless optical communications.

1. Introduction

Many subsea industrial, military and scientific activities such as oceanographic surveying, or the control, monitoring and maintenance of subsea infrastructure, require the transfer of increasingly large amounts of data through high-speed communications. For example, unmanned and autonomous underwater vehicles (UUVs and AUVs) are used to capture high-resolution images or videos for applications such as assessing subsea oil and gas infrastructure. In this example,

the captured image and video data would require to be transferred back to a surface vessel for assessment, with navigation commands and instructions being sent to the vehicles. While high-speed data links can be achieved using underwater cables or tethers, this can be impractical, expensive or in some cases restrictive due to the challenging underwater environment. Therefore, high-speed underwater wireless links are greatly desirable.

Acoustic technologies are the most widely used form of underwater wireless communications due to their long range covering distances up to tens of kilometers [1]. However, they suffer from low data rates (in the order of kb/s) because of their limited bandwidth (around tens of kHz) [2]. Moreover, acoustics suffer from low speed and multipath propagation which may lead to inter-symbol interference (ISI) [3]. Radio Frequency (RF) communications, despite their widespread deployment over free-space (e.g., cell phones, TV, radio, satellite communications), are not readily deployable underwater as electromagnetic (EM) waves at these frequencies are heavily attenuated by seawater [4]. As such, underwater RF wireless communications require high transmission power and complex antenna designs [5] and yet are limited to short distances (on the order of meters) [6].

Underwater wireless optical communication (UWOC) may be considered as an alternative to acoustics and RF as the attenuation of light by water is lowest in the visible region [7]. The last 20 years has also witnessed the rapid development of efficient, compact and robust solid-state transmitters (light-emitting diodes (LEDs) and laser diodes) emitting light in the violet-blue-green region of the visible spectrum, as well as highly-sensitive photoreceivers such as single-photon avalanche diodes. Therefore, high-speed underwater optical data transmission over tens of meters using visible wavelengths is now feasible. For example, recent reports by Li *et al.* showed the demonstration of 25 Gb/s by using a vertical-cavity surface-emitting laser (VCSEL) at 680 nm for 5 m [8]. Fei *et al.*, using a blue laser diode, demonstrated 16.6 Gb/s for 5 m and 6.6 Gb/s over 55 m of clear tap water [9] while an RGB (Red Green Blue) laser was used by Kong *et al.* to achieve 9.51 Gb/s for 10 m [10].

LEDs have attracted a great deal of attention in recent years for use as light-fidelity (Li-Fi) transmitters, where LED luminaires are used to provide both general purpose lighting and mb/s or Gb/s optical wireless links. LEDs have also been demonstrated as transmitters in underwater optical links. Recent results by Shi *et al.* showed the demonstration of 15.17 Gb/s over 1.2 m of clear tap water by employing 5 LEDs of primary colors [11]. A single green LED operating at 521 nm was used by Wang *et al.* to demonstrate 2.175 Gb/s through 1.2 m of clear tap water [12]. LEDs are relatively simple, and cost-effective in comparison with other sources such as lasers, however standard off-the-shelf LEDs have limited modulation bandwidth, typically 20 mHz or so, due to the large capacitance of standard LED dies, which limits the achievable data rates. Micro-sized light-emitting diodes (μLEDs) on the other hand have much smaller dimensions (typically ≤ 100 μm) and therefore their bandwidths are not limited by device capacitance. For example, we previously reported violet-emitting μLEDs with modulation bandwidths up to 655 mHz, using which wireless data rates of up to 7.91 Gb/s over free-space were demonstrated [13]. μLEDs have been employed for UWOC. For example, Tian *et al.* reported 800 mb/s over 0.6 m and 200 mb/s over 5.4 m of clear tap water [14] using a single μLED at 450 nm. However, the small active area of μLEDs results in a relatively low output power from a single μLED ($<$5 mW), which may be insufficient for practical UWOC due to absorption and scattering in an underwater environment.

In order to mitigate this, here we report the deployment of series-connected μLED arrays operating at 450 nm for UWOC. These devices consist of 6 μLED pixels, of either 60 or 80 μm in diameter and connected in series. This allows the device to achieve higher optical power than a single μLED pixel while retaining the characteristic high modulation bandwidth of μLEDs. As a result, these devices offer the high output powers of a standard LED die, but with the high modulation bandwidth of μLEDs. Using orthogonal frequency division multiplexing (OFDM), data rates of up to 4.92 Gb/s, 3.22 Gb/s and 3.4 Gb/s over 1.5 m, 3 m and 4.5 m, respectively, with corresponding bit error ratios (BERs) of 1.5×10^{-3}, 1.1×10^{-3} and 3.1×10^{-3}, of clear tap water are here demonstrated. Furthermore, by adding a scattering agent to clear tap water we explored the performance of these optical links through water of varying turbidities. Mb/s data transmission was demonstrated over 5.33 attenuation lengths. These results demonstrate that the relatively high
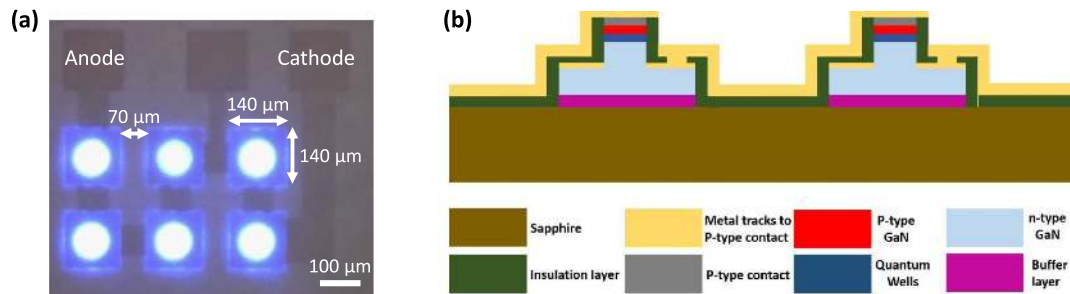
Fig. 1. (a) Planview optical image of six pixels from the μLED array at a DC operating current of 1 mA. (b) Schematic cross-section of two adjacent elements of the series-biased μLED array.

bandwidth and output power of these series-connected μLEDs can be used to achieve high data rates and/or mitigate the effects of signal attenuation.

2. μLED Design, Fabrication and Characterization

The μLED devices reported here were fabricated from commercial blue-emitting III-nitride LED wafers grown on a 2" c-plane sapphire substrate with periodically patterned surfaces. The fabrication procedure is similar to that described in [15] and [16], which is summarized as follows. Standard photolithography and etching techniques were used to etch down to the n-GaN layer to define disk-shaped μLED pixels. A further processing step etched down to the sapphire substrate to electrically-isolate each of these μLEDs on individual 140 $\times$ 140 μm^2 mesas, with a 70 μm spacing between adjacent mesas (Fig. 1(a)). P-type and N-type contact metals (Pd and Ti/Au) were then deposited, interconnecting the μLEDs in series. Fig. 1(b) illustrates the simplified cross-sectional structure of the series-connected μLED array, where two adjacent μLEDs elements are shown as an example and the electrical interconnections between them are highlighted.

Each μLED pixel shown here is of either 60 μm or 80 μm in diameter while the center wavelength is approximately 450 nm for all devices. As shown in Fig. 1(a), each device consists of 6 μLED pixels arranged in a 3 $\times$ 2 array. In this work all 6 pixels were simultaneously driven together in series in order to maximize the output power.

For the series-connected devices with respectively 60 μm and 80 μm pixels, Fig. 2(a) presents the current versus voltage (I-V) and the output optical power versus current (L-I) while Fig. 2(b) shows the -3 dB electrical-to-electrical (E-E) and electrical-to-optical (E-O) bandwidths versus current characteristics. Optical power is the forward detected output and was measured by placing the μLEDs in close proximity to a calibrated Si photodiode. The bandwidths were measured as detailed previously [15]. As shown, the turn-on voltage at 1 mA for the 60 μm in diameter device is 21.7 V corresponding to about 3.6 V for each μLED element whereas for the 80 μm device the turn-on voltage is 20 V corresponding to about 3.3 V for each μLED element. Additionally, both devices can be operated at a current beyond 50 mA and demonstrate an optical power before thermal rollover of over 21 mW and 15 mW for the 80 μm and 60 μm device, respectively.

In our previous work we have shown that in a single μLED emitter [16], [17] the differential carrier lifetime decreases as the current density increases and leads to an increase of the E-O bandwidth of the device [18]. As can be seen in Fig. 2(b), the E-O bandwidth for the 60 μm in diameter series-connected μLED array is 338.5 mHz at 30 mA whilst for the 80 μm device it is 263 mHz at 50 mA. These trends are in agreement with previous work [19] where it was observed that as the pixel diameter of a μLED element decreases, the corresponding E-O bandwidth increases.
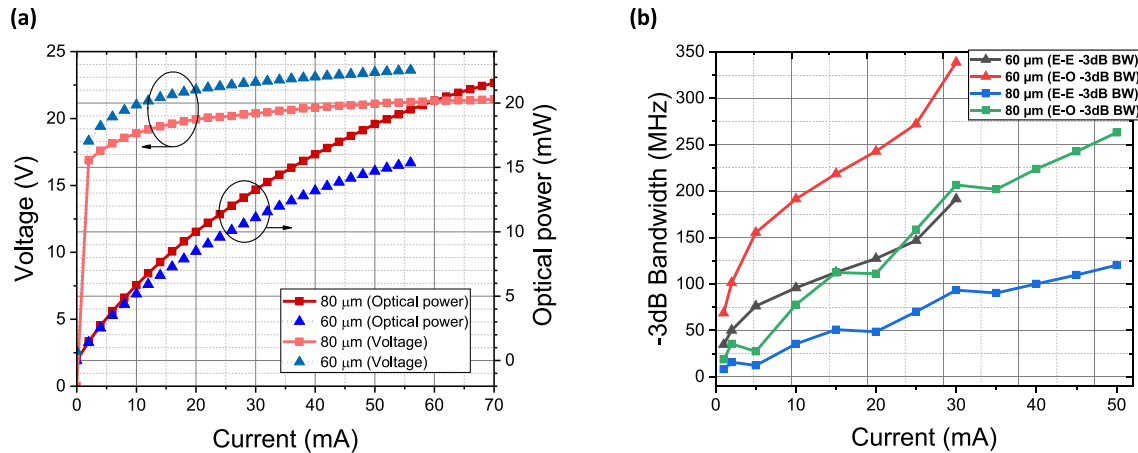
(a)

(b)

Fig. 2. (a) I-V, L-I, and (b) −3 dB bandwidth plots for the two respective devices comprising six 60 μm and 80 μm μLEDs in series.

3. Water Sample Characterization

In natural waters two fundamental wavelength dependent processes are mainly responsible for the optical attenuation of light, namely absorption and scattering, whose coefficients are denoted as $\alpha(\lambda)$ and b(λ), respectively, both with units of m^{-1}. We may then relate the attenuation of optical power to the path length z [20], [21]:

$$P_R(z) = P_T e^{-c(\lambda) \cdot z} \tag{1}$$

where c(λ) = $\alpha(\lambda)$ + b(λ) is the overall beam attenuation and P_R and P_T are the received and transmitted powers, respectively. Eq. (1) allows the power received at a distance z to be estimated, assuming that scattered photons do not reach the receiver and thus do not contribute to the final received power. We also define the attenuation length (AL) of a water sample as the distance at which the received power in a water sample is reduced to 1/e of the transmitted power, and it is equal to 1/c(λ) [22]. The number of attenuation lengths through which transmitted light propagates is given as the unit-less product c(λ)·z [21].

Following a method commonly reported [21], [23]–[26] in this work a mixture of aluminum and magnesium hydroxide was used as a scattering agent (Maalox antacid) and added to clear tap water to vary the level of attenuation. Increasing the concentration of Maalox increases the amount of scattering and thereby the attenuation of the optical signal as it propagates through the water. While this approach does not model affects such as turbulence, it is a simple method to mimic different natural water analogs in a laboratory setting. Detailed studies by other groups on the effect of turbulence are available elsewhere [27].

The relationship between Maalox concentration and c(λ) was measured as follows. Nine different concentrations of Maalox were examined, ranging from 0.000625% (1 ml of Maalox in 160 l of tap water) to 0.005625% (9 ml of Maalox). To estimate c(λ) at each concentration, the optical beam from a blue laser diode (Osram, PL450B) operating at the same nominal central wavelength as the μLEDs (450 nm), was propagated through the 1.5 m length of our water tank (dimensions 1.5 m × 0.35 m × 0.35 m). A laser was chosen for these measurements as the divergence of the μLED emission would make accurate estimation of c(λ) difficult. A plastic aspheric lens (Thorlabs, CAY033), was placed in front of the laser diode to collimate the beam which was subsequently focused onto a power meter sensor (Thorlabs, S121C), located at the other side of the tank. The received optical power, P_R, at each concentration was measured. Using these values for P_R along with Eq. (1) and the measured transmitted power of P_T, the corresponding attenuation coefficients for each water sample were calculated and are shown in Fig. 3(a). It can be seen that
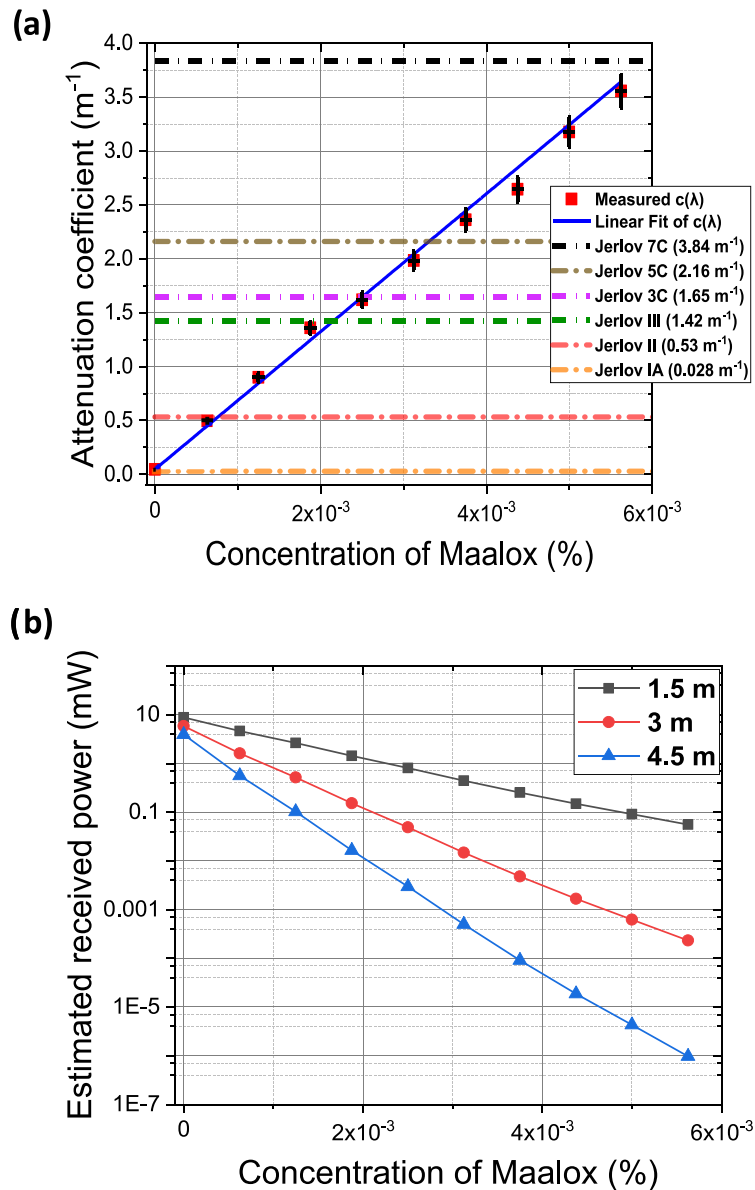
(a)

(b)

Fig. 3. (a) The calculated attenuation coefficients versus the content of the scattering agent (Maalox). For comparison, the typical values of six Jerlov ocean types are given as defined by [26], [27]. (b) The estimated received power over 1.5 m, 3 m and 4.5 m versus the Maalox concentration.

the minimum measured attenuation coefficient, which corresponds to clear tap water (no Maalox added) is 0.05 m^{-1}, a value relatively close to that of Jerlov IA open ocean water type which is 0.028 m^{-1} [28], [29]. For the samples with added Maalox, the maximum measured attenuation coefficient was 3.56 m^{-1} for 0.005625% (9 ml) of Maalox, and is close to the Jerlov 7C coastal ocean type where c(450) = 3.84 m^{-1} [28], [29].

Fig. 3(b) illustrates the estimated received power for the 80 μm-in-diameter series-connected μLED array, for each concentration of the scattering agent at 1.5 m, 3 m and 4.5 m. The estimated received power, P_R, was calculated through Eq. (1) and by taking into account that the estimated transmitted power, P_T, was 13.27 mW at 30 mA, based on the L-I measurements in Fig. 2(a).
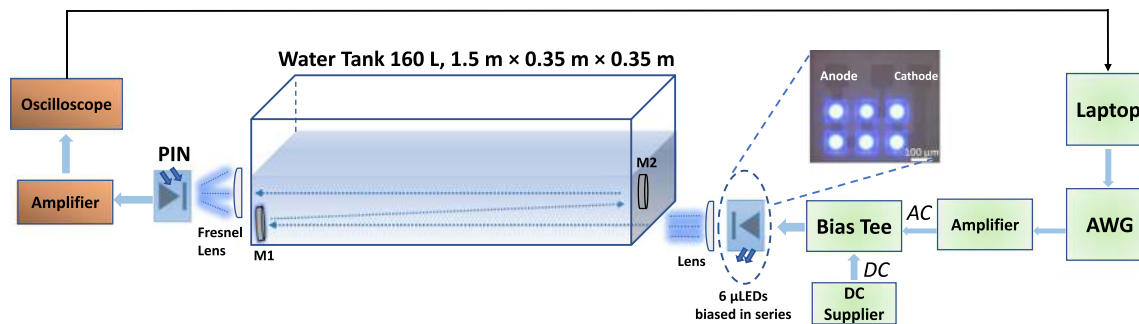
Fig. 4. Illustration of the experimental set-up used for the UWOC measurements of this work. Two mirrors (M1 and M2) were placed appropriately to increase the optical link from 1.5 m up to 3 m and 4.5 m.

4. Data Transmission and Experimental Set-Up

The data transmission experimental set-up is depicted in Fig. 4. The digital data signal to be transmitted was generated and processed in MATLAB. Afterwards, this optimized signal was converted to analog through an arbitrary waveform generator (AWG, Agilent, 81180A) and amplified (amplifier SHF S126A). The signal was combined with a DC current of 30 mA through a bias tee (Tektronix, PSPL5575A) to drive the μLED arrays.

A condenser lens (Thorlabs, ACL50832U-A) was used to collimate the beam to be optically transmitted through the 1.5 m long water tank. For the longer range data transmissions two 100 mm diameter mirrors (M1 and M2) were mounted appropriately in the tank to increase the optical path up to 3 m and 4.5 m. At the receiver end, a 4-inch in diameter Fresnel lens (Edmund Optics, #46-614) was used to focus the collimated beam onto a PIN photoreceiver of 1.4 GHz bandwidth (Femto, HAS-X-S-1G4-SI). The amplification of the received signal was processed through an amplifier (Mini-Circuits, ZHL-6A-S+) and captured through an oscilloscope (Agilent, MSO 7104B). The received signal was processed and demodulated offline in MATLAB. At this stage, the transmitted data and received data is compared to identify any incorrectly transmitted bits, allowing the BER to be calculated. It should be noted that OFDM is robust against multi-path effects of the sort that would be experienced in underwater environments. A more detailed description of the OFDM data modulation process can be found in our previous work [13], [30].

5. Communication Performance Results

As with our previous work [13], [30], an adaptive bit and energy loading scheme was used to allow different Quadrature Amplitude Modulation (QAM) levels to loaded onto the OFDM subcarriers based on the measured signal-to-noise ratio (SNR) of each carrier. The higher the carrier SNR, the higher the QAM level that could be used and thus the more bits could be loaded onto that channel. This is illustrated in Fig. 5 where an example of the measured SNR and corresponding number of transmitted bits per OFDM carrier frequency is shown for a transmission measurement taken using a 60 μm in diameter series-connected μLED device over 1.5 m of clear tap water.

Fig. 6 shows the measured BER against various transmission data rates by employing the 60 μm in diameter series-connected μLEDs as transmitter, through 1.5 m of clear water. The red dashed line indicates the BER target of 3.8×10^{-3} [31], below which "error-free" data transmission can be achieved using Forward Error Correction (FEC) with a 7% overhead of the gross data rate. The maximum achieved data rate that met this criterion was 4.92 Gb/s which corresponds to a net data rate of 4.58 Gb/s after FEC, though it should be pointed out that FEC was not actually used in this work.
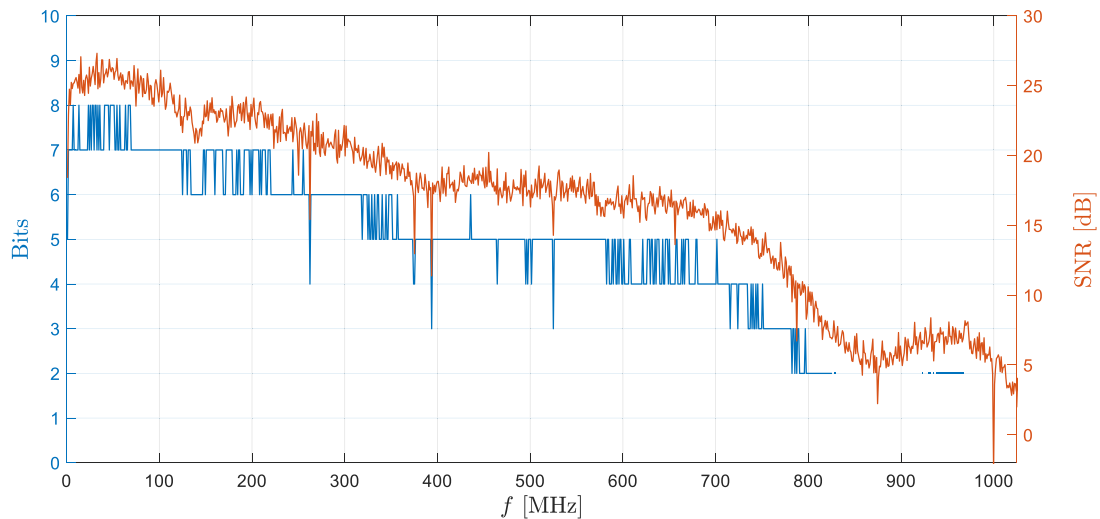
Fig. 5. Measured SNR (orange) and corresponding bit loading (blue) versus OFDM carrier frequency, obtained using a 60 μm in diameter series-connected μLED device over 1.5 m of clear tap water.
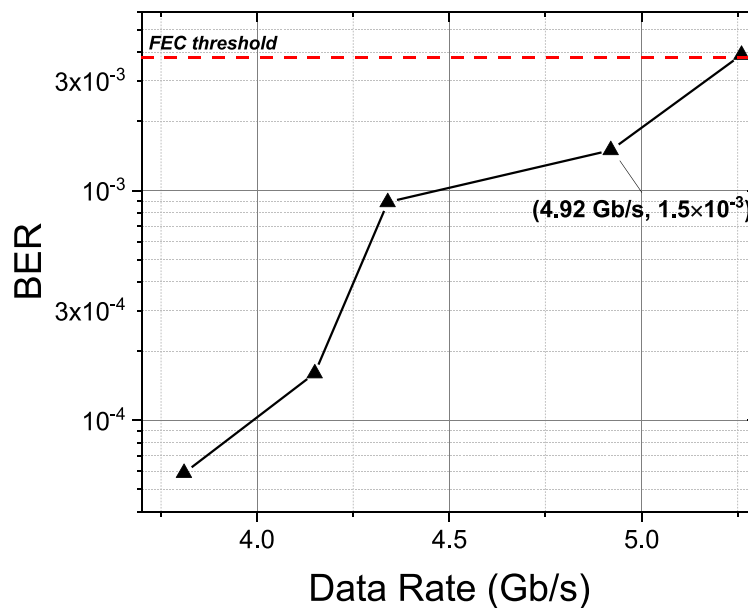

Fig. 6. BER versus data rate for the 60 μm μLEDs in series. Transmission is over 1.5 m of clear tap water ($c(450) = 0.05$ m^{-1}).

Fig. 7(a) shows the BER vs. data rates for the 80 μm in diameter series-connected μLEDs through different water turbidities, as described in Section 3, over 1.5 m. The maximum data rate through clear tap water is 3.78 Gb/s at a BER of 3.7×10^{-3} and it can be shown that the increase in water turbidity, leads to attenuated transmission power levels collected by the detector and causes a lower overall signal-to-noise ratio (SNR) level. With a lower SNR level, fewer bits are loaded on each subcarrier and the achievable data rate decreases. In extreme water turbidities ($c(450) = 3.56$ m^{-1}) a data rate up to 15 mb/s was demonstrated over 5.33 ALs.
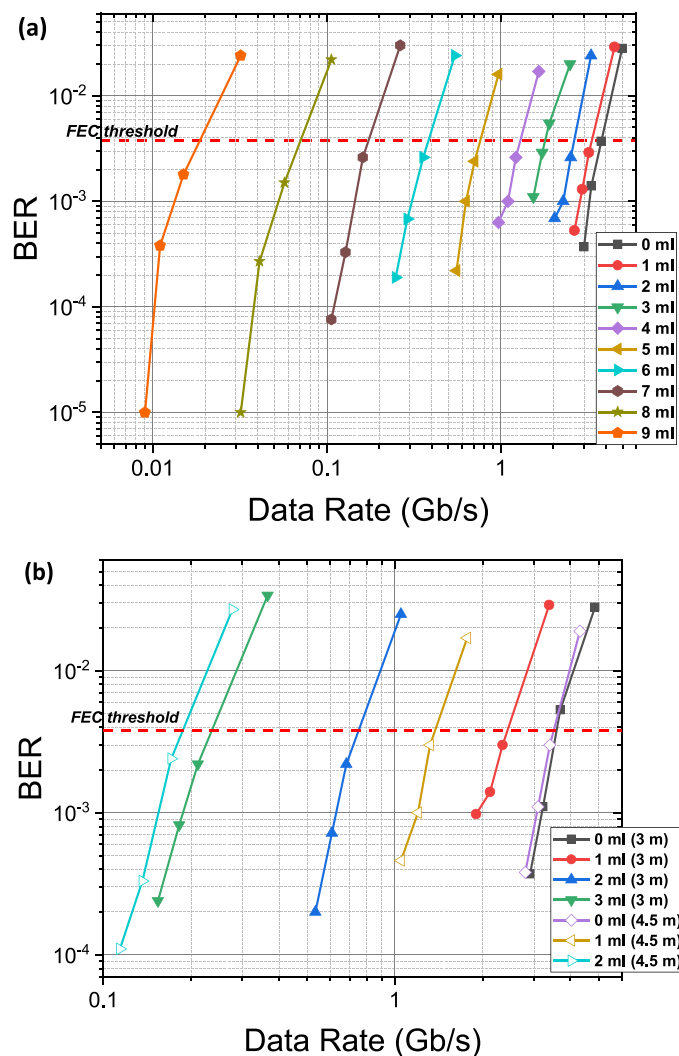
Fig. 7. (a) BER vs. data rate for the 80 μm in diameter series-connected μLEDs through different water turbidities over 1.5 m. (b) BER vs. data rate for the same device through different water turbidities over 3 m and 4.5 m. Note that the maximum error-free data rates were obtained at slightly different BERs.

Fig. 7(b) presents the BER vs. data rate for the same device at the ranges of 3 m and 4.5 m through different concentrations of Maalox. At 3 m the maximum data rate through clear tap water is 3.22 Gb/s with a BER of 1.1×10^{-3} while at 4.5 m a larger BER of 3.1×10^{-3} is achieved for 3.4 Gb/s (corresponding c(450) = 0.05 m^{-1} for both ranges). As the Maalox concentration increases, the maximum data rate drops to 211 mb/s at 3 m over 4.08 ALs with a BER of 2.3×10^{-3} (corresponding c(450) = 1.36 m^{-1}) and to 171 mb/s at 4.5 m over 4.05 ALs with a BER of 2.5×10^{-3} (corresponding c(450) = 0.90 m^{-1}).

The drop in data rate at all ranges can be explained by taking into account the Shannon-Hartley theorem [32]:

$$D = B \log_2 \left(1 + S/N\right) \tag{2}$$

where D is the maximum data transmission rate in bits/sec, B is the channel bandwidth in Hz, S is the average signal power over the entire bandwidth in W, N is the average noise power over the entire bandwidth at the Rx in W while S/N is the SNR. The degradation of the received SNR and
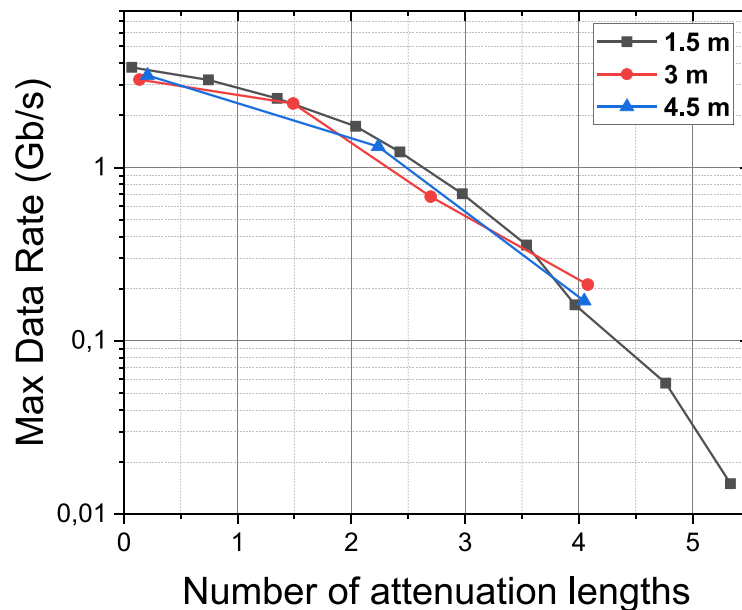
Fig. 8. The maximum data rates vs. the number of attenuation lengths for all ranges examined in this work (1.5 m, 3 m, 4.5 m).

the received optical power due to the increased attenuation result in a decrease in the achievable data rates.

Fig. 8 illustrates the error-free maximum data rates versus the number of ALs for all transmission distances. It can be seen that the maximum data rate decreases with an increase in the number of ALs, for all path lengths. This can be understood as the increased attenuation of the signal results in a lower SNR. It can also be seen that similar data rates are obtained when the number of ALs is similar, although the curves do not overlap exactly because each maximum data rate was obtained at a slightly different BER as shown in Fig. 7(a) and (b).

These results indicate that the relatively high power and bandwidth available from series-connected μLEDs can enable UWOC at Mb/s or Gb/s, even through turbid water samples. In future, further improvements to the achievable data rates and/or link lengths could be obtained by, for example, increasing the transmitted power by adding additional LEDs, narrowing the optical beam profile, or applying multiplexing techniques such as wavelength division multiplexing (WDM).

6. Conclusion

In this work, the high output power and modulation bandwidth of μLED arrays, consisting respectively of 6 series-connected pixels of diameter 60 μm or 80 μm, enabled Gb/s underwater optical wireless data transmissions using OFDM as modulation scheme, over three underwater distances of 1.5 m, 3 m and 4.5 m. A BER of 1.5×10^{-3} was achieved for a maximum data rate of 4.92 Gb/s through 1.5 m of clear tap water whose attenuation coefficient was $c(450) = 0.05$ m^{-1}. Further underwater wireless optical transmissions were performed through different water turbidities: 2.34 Gb/s were demonstrated for an attenuation coefficient of 0.5 m^{-1} which is close to Jerlov II open ocean type (0.53 m^{-1}) over 3 m, whereas 1.32 Gb/s were shown over 4.5 m. With an attenuation coefficient of 3.56 m^{-1} and over 5.33 ALs, a data rate of 15 mb/s was achieved through 1.5 m. Our approach is compatible with multi-wavelength operation for WDM, and this is currently under investigation. The results of this work show the potential implementation of series-connected μLEDs to enable high-speed underwater wireless communications through various water turbidities.

Acknowledgment

References

[1] E. M. Sozer, M. Stojanovic, and J. G. Proakis, "Underwater acoustic networks," *IEEE J. Ocean. Eng.*, vol. 25, no. 1, pp. 72–83, Jan. 2000.

[2] P. Lacovara, "High-bandwidth underwater communications," *Marine Technol. Soc. J.*, vol. 42, no. 1, pp. 93–102, 2008.

[3] M. Stojanovic, "High-speed underwater acoustic communications," in *Underwater Acoustic Digital Signal Processing and Communication Systems*, Boston, MA, USA: Springer, 2013, pp. 1–35.

[4] J. R. Apel, *Principles of Ocean Physics*, vol. 38. New York, NY, USA: Academic, 1988.

[5] A. I. Al-Shamma'a, A. Shaw, and S. Saman, "Propagation of electromagnetic waves at MHz frequencies through seawater," *IEEE Trans. Antennas Propag.*, vol. 52, no. 11, pp. 2843–2849, Nov. 2004.

[6] C. Uribe and W. Grote, "Radio communication model for underwater WSN," in *Proc. 3rd Int. Conf. New Technol. Mobility Secur.*, 2009, pp. 1–5.

[7] B. Wozniak, *Light Absorption in Sea Water*. New York, NY: Springer, 2006.

[8] C. Y. Li *et al.*, "A 5 m/25 Gbps underwater wireless optical communication system," *IEEE Photon. J.*, vol. 10, no. 3, Jun. 2018, Art. no. 7904909.

[9] C. Fei *et al.*, "16.6 Gbps data rate for underwater wireless optical transmission with single laser diode achieved with discrete multi-tone and post nonlinear equalization," *Opt. Express*, vol. 26, no. 26, 2018, Art. no. 34060.

[10] M. Kong *et al.*, "10-m 951-Gb/s RGB laser diodes-based WDM underwater wireless optical communication," *Opt. Express*, vol. 25, no. 17, 2017, Art. no. 20829.

[11] Y. Zhou *et al.*, "Common-anode LED on Si substrate for beyond 15 Gbit/s underwater visible light communication," *Photon. Res.*, vol. 7, no. 9, pp. 1019–1029, 2019.

[12] F. Wang, Y. Liu, F. Jiang, and Nan Chi, "High speed underwater visible light communication system based on LED employing maximum ratio combination with multi-PIN reception," *Opt. Commun.*, vol. 425, pp. 106–112, 2018.

[13] R. X. G. Ferreira *et al.*, "High bandwidth GaN-based micro-LEDs for multi-Gb/s visible light communications," *IEEE Photon. Technol. Lett.*, vol. 28, no. 19, pp. 2023–2026, Oct. 2016.

[14] P. Tian *et al.*, "High-speed underwater optical wireless communication using a blue GaN-based micro-LED," *Opt. Express*, vol. 25, no. 2, pp. 1193–1201, 2017.

[15] E. Xie *et al.*, "High-speed visible light communication based on a III-nitride series-biased micro-LED array," *J. Lightw. Technol.*, vol. 37, no. 4, pp. 1180–1186, Feb. 2019.

[16] E. Xie *et al.*, "Design, fabrication, and application of GaN-based micro-LED arrays with individual addressing by N-electrodes," *IEEE Photon. J.*, vol. 9, no. 6, Dec. 2017, Art no. 7907811.

[17] J. J. D. McKendry *et al.*, "High-speed visible light communications using individual pixels in a micro light-emitting diode array," *IEEE Photon. Technol. Lett.*, vol. 22, no. 18, pp. 1346–1348, Sep. 2010.

[18] S. Rajbhandari *et al.*, "A review of gallium nitride LEDs for multi-gigabit-per-second visible light data communications," *Semicond. Sci. Technol.*, vol. 32, no. 2, 2017, Art. no. 023001.

[19] J. J. D. McKendry *et al.*, "Visible-light communications using a CMOS-controlled micro-light-emitting- diode array," *J. Lightw. Technol.*, vol. 30, no. 1, pp. 61–67, Jan. 2012.

[20] M. N. Berberan-Santos, "Beer's law revisited," *J. Chem. Educ.*, vol. 67, no. 9, pp. 757–759, 1990.

[21] W. Cox and J. Muth, "Simulating channel losses in an underwater optical communication system," *J. Opt. Soc. Am. A*, vol. 31, no. 5, pp. 920–934, 2014.

[22] T. Petzold, "Volume scattering functions for selected ocean waters," *Scripps Inst. Ocean.*, no. 3, pp. 72–78, 1972.

[23] A. Laux *et al.*, "The a, b, cs of oceanographic lidar predictions: A significant step toward closing the loop between theory and experiment," *J. Modern Opt.*, vol. 49, no. 3–4, pp. 439–451, 2002.

[24] B. M. Cochenour, L. J. Mullen, and A. E. Laux, "Characterization of the beam-spread function for underwater wireless optical communications links," *IEEE J. Ocean. Eng.*, vol. 33, no. 4, pp. 513–521, Oct. 2008.

[25] B. Cochenour, L. Mullen, and J. Muth, "Effect of scattering albedo on attenuation and polarization of light underwater," *Opt. Lett.*, vol. 35, no. 12, pp. 2088–2090, 2010.

[26] B. Cochenour, S. O'Connor, and L. Mullen, "Suppression of forward-scattered light using high-frequency intensity modulation," *Opt. Eng.*, vol. 53, no. 5, 2013, Art. no. 051406.

[27] Z. Vali, A. Gholami, Z. Ghassemlooy, M. Omoomi, and D. G. Michelson, "Experimental study of the turbulence effect on underwater optical wireless communications," *Appl. Opt.*, vol. 57, no. 28, pp. 8314–8319, 2018.

[28] N. G. Jerlov, *Marine Optics*, vol. 14. Amsterdam, The Netherlands: Elsevier, 1976.

[29] M. G. Solonenko and C. D. Mobley, "Inherent optical properties of Jerlov water types," *Appl. Opt.*, vol. 54, no. 17, pp. 5392–5401, 2015.

[30] D. Tsonev *et al.*, "A 3-Gb/s single-LED OFDM-based wireless VLC link using a gallium nitride micro-LED," *IEEE Photon. Technol. Lett.*, vol. 26, no. 7, pp. 637–640, Apr. 2014.

[31] I.-T. S. Group, "Forward error correction for high bit-rate DWDM submarine systems," ITU-T Rec. G.975.1 (02/2004), 2005.

[32] C. E. Shannon, "A mnathematical theory of communication, Part I, Part II," *Bell Syst. Tech. J.*, vol. 27, pp. 623–656, 1948.